Remanent magnetization of the dilute antiferromagnets $Mn_{1-x}Zn_xF_2$ at very low magnetic fields

1993 J. Phys.: Condens. Matter 5 8083

(http://iopscience.iop.org/0953-8984/5/43/020)

J. Phys.: Condens. Matter 5 (1993) 8083–8096. Printed in the UK

Remanent magnetization of the dilute antiferromagnets $Mn_{1-x}Zn_xF_2$ at very low magnetic fields

T Fries†, Y Shapira†, A Paduan-Filho‡, C C Becerra‡ and F Palacio§

† Department of Physics, Tufts University, Medford, MA 02155, USA

‡ Instituto de Física, Universidade de São Paulo, CP 20516, São Paulo, SP, Brazil

§ Instituto de Ciencia de Materiales de Aragón, CSIC, Universidad de Zaragoza, E-50 009, Zaragoza, Spain

Received 24 June 1993, in final form 2 August 1993

Abstract. The magnetization of $Mn_{1-x}Zn_xF_2$ single crystals with $x = 0.25$ and 0.51 was studied in low magnetic fields directed along the easy axis (c axis). Data were taken for axial fields H_{axial} between $\sim 10^{-3}$ Oe and ~ 10 Oe. Below the Néel temperature T_N, the magnetization M for given H_{axial} and temperature T depended on the history of the sample. Data obtained while cooling in a constant H_{axial} (FC procedure) show a dramatic rise of M below T_N. This rise corresponds to the development of a thermoremanent magnetization M_r. The sign and magnitude of M_r depend on the axial field present while cooling; M_r is proportional to H_{axial} at low axial fields, but approaches saturation at $H_{axial} \sim 1$ Oe. The measured values of $M_r(t)/M_r(0)$, where $t = T/T_N$ is the reduced temperature, are independent of H_{axial} and are the same for both samples. They also agree with values of $M_r(t)/M_r(0)$ measured in $K_2Fe_{1-x}In_xCl_5{\cdot}H_2O$, but not with those measured in $K_2Fe(Cl_{1-x}Br_x)_5{\cdot}H_2O$. Fits of the temperature dependence of M_r near T_N yield an effective critical exponent β_r. Extrapolated values of β_r very close to T_N are between 0.35 and 0.40. Experiments in which H_{axial} is changed below T_N show that the remanent magnetization is controlled only by the field $H_{axial}(T_N)$ present while cooling through T_N. The observed properties of M_r, particularly the saturation in axial fields of ~ 1 Oe, cannot be explained in terms of domains caused by random fields. Another explanation that fails is based on the statistical difference between the number of up and down spins in each of the antiferromagnetic domains, which exist even in the absence of random fields. It is possible that M_r arises from the walls between such domains, but since this explanation is yet to be tested other possible explanations cannot be ruled out.

1. Introduction

Recently we reported the observation of a remanent magnetization in several disordered antiferromagnets at very low magnetic fields [1, 2]. This low-field remanent magnetization had striking new features that had not been observed previously, e.g., saturation in fields as low as ~ 1 Oe. All the materials studied in [1] and [2] were disordered low-anisotropy uniaxial antiferromagnets. In the present paper we give a much fuller account of the results in $Mn_{1-x}Zn_xF_2$. Detailed results for the other disordered antiferromagnets discussed in [1] and [2] will be presented later.

Disordered uniaxial antiferromagnets have been studied extensively in recent years, primarily because they allow tests of important theoretical models such as the random-field Ising model [3]. Among the many properties that have been studied is the remanent magnetization. In an early study Ikeda and Kikuta [4] observed the remanent magnetization of $Mn_{1-x}Zn_xF_2$ in magnetic fields $H \geqslant 50$ Oe. Later, the remanent magnetization was studied in other materials, but at still higher magnetic fields [5, 6]. In all these studies the

0953-8984/93/438083+14$07.50

remanent magnetization was attributed to random fields. In contrast, The low-field remanent magnetization discussed in the present paper appears not to be related to random fields.

The precise meaning of 'remanent magnetization' depends on the experimental procedure that is followed. Among the different types of remanent magnetization are the thermoremanent magnetization (TRM), the isothermal remanent magnetization (IRM) and the excess magnetization ΔM. The TRM is the magnetization obtained by cooling in a magnetic field, starting above the Néel temperature T_N, and then reducing the field to zero. The TRM is a function of the field H at which the sample is cooled and of the final temperature T at which the field is reduced to zero. The IRM is the magnetization obtained by cooling in zero field, then applying a magnetic field isothermally, and finally reducing the field to zero at the same temperature. The excess magnetization ΔM is the *difference* between the magnetizations obtained by (1) cooling in a magnetic field (FC) and (2) cooling in zero field and then applying the field (ZFC). That is, $\Delta M = M_{FC} - M_{ZFC}$, where both M_{FC} and M_{ZFC} are measured at the same H and T. These three specific types of remanent magnetization can, and often do, differ from each other. Much of the earlier work on disordered antiferromagnets focused on the excess magnetization [4–6], although the TRM and IRM were also measured [6]. As discussed later, the TRM and the excess magnetization ΔM turn out to be equal in the present study, which was carried out at very low magnetic fields ($H \lesssim 10$ Oe). What is loosely called 'remanent magnetization' in the early parts of this paper is later identified as the TRM, which is in turn equal to ΔM.

MnF_2 has a rutile crystal structure, with a tetragonal symmetry. Magnetically, the material is an easy-axis antiferromagnet, with two interpenetrating sublattices. The anisotropy field is of the order of 1% of the exchange field, and the tetragonal axis (c axis) is the easy axis. These properties also apply to $Mn_{1-x}Zn_xF_2$ above the percolation limit. Because of its simple crystal and magnetic structures, $Mn_{1-x}Zn_xF_2$ has been a favourite model system for experimental studies of low-anisotropy random-site antiferromagnets.

2. Experimental details

Two single crystals of $Mn_{1-x}Zn_xF_2$ were used. These were cut from boules grown several years ago by D Gabbe at MIT. The Czochralski method was used. Crystals from the same boules were used previously in studies of effects caused by random fields [7–12]. The Zn concentrations in these boules, determined by atomic absorption, were $x = 25\%$ and 51%. The two single crystals used here had linear dimensions of several mm.

Magnetization data were taken with a SQUID magnetometer system manufactured by Quantum Design. The power supply that is part of that system, however, was replaced by a Keithley model 225 current source, which allowed a finer control of the current through the superconducting solenoid magnet. To minimize trapped-flux effects the magnetic field H was kept below 23 Oe, following a cool down of the magnet from above its superconducting transition temperature. For these low fields, H was a reproducible function of the current I through the solenoid.

The magnetometer system allowed measurements of both the 'longitudinal' magnetic moment along the bore of the solenoid, and the 'transverse' moment along one fixed direction perpendicular to the bore. The remanent moment along any transverse direction in the sample could be measured by rotating the sample about the longitudinal axis.

Each sample was mounted with the c axis (which is the antiferromagnetic easy axis) along the bore of the solenoid. The misalignment error was $\lesssim 1°$. Thus, the longitudinal component of H along the bore, was very nearly equal to the axial component H_{axial} along

the easy axis. This H_{axial} was controlled by the current I through the magnet. The I–H_{axial} characteristic below 23 Oe, which was linear, was calibrated repeatedly by measuring the longitudinal magnetization of a sample of superconducting indium at 2 K. The calibration assumed a complete Meissner effect, and included a correction for the demagnetization factor. Various checks of this 'indium calibration' have already been discussed in [1]. The precision of this calibration was about 0.001 Oe, and the accuracy was 2%.

The indium calibration had a small offset error. The current I corresponding to $H_{axial} = 0$ was slightly in error, which was equivalent to a constant shift of the values of H_{axial}. The magnitude of the shift was about 0.01 Oe. The evidence suggested that this shift was caused by the ever-present transverse component of the earth field, $H_{E\perp} \sim 0.1$ Oe. (This $H_{E\perp}$ could not be cancelled by passing current through the magnet.) The transverse earth field affected the indium calibration of H_{axial} in two ways: (1) because the c axis was not perfectly aligned with the longitudinal direction of the magnet's bore, $H_{E\perp}$ had a finite projection on the c axis; and (2) the transverse magnetic moment of the indium sample, arising in response to $H_{E\perp}$, led to a very small, but finite, spurious signal for the longitudinal moment of that sample. The latter 'crosstalk' between the transverse moment and the measured longitudinal signal was caused by an instrumental imperfection. As discussed later, there is strong evidence that the thermoremanent magnetization of $Mn_{1-x}Zn_xF_2$ reverses its sign at $H_{axial} = 0$. Assuming that the sign reversal is exactly at $H_{axial} = 0$, the small error in the zero position of H_{axial} could be corrected to an accuracy of 0.001 Oe. When necessary we will distinguish between the uncorrected and corrected indium calibrations.

The Quantum Design magnetometer system was used to control and measure the temperature T. To assure better temperature equilibration, 5–15 min delays were programmed between successive temperatures in addition to the automatic delays of the system. The lengths of the additional delays were based on a study of the temperature equilibration in the system. That study, which was performed by us previously, indicates that the accuracy of T in the range covered in the present work was better than 0.1 K.

After all the data below 23 Oe were taken on a given sample, additional magnetization data were taken at 2.0 and 4.0 kOe. For these much higher fields, the standard magnet supply of the Quantum Design magnetometer system was used.

3. Experimental results

3.1. Magnetization rise below T_N

Magnetization data were taken as a function of T at fixed H_{axial}. Most data were for the longitudinal magnetization, which is virtually identical to the axial magnetization, along the easy axis. Only a few data for the transverse magnetization were taken. Unless otherwise stated the results are always for the longitudinal (axial) magnetization.

Data were first taken while cooling from above the Néel temperature at a constant H_{axial} (FC data). After reaching the lowest temperature, more data were usually taken while heating in the same field (FH data). Typical results for $x = 0.51$ and 0.25 are shown in figures 1 and 2, respectively. Note that the FC and FH data at the same field are practically identical. The most striking feature in figures 1 and 2 is the rise in the magnetization M when the sample is cooled through the Néel temperature, $T_N = 20.3$ K for $x = 0.51$, and 46.0 K for $x = 0.25$. As discussed later, the rise of M is due to the development of a remanent magnetization below T_N. The magnetization rise below T_N is quite pronounced even at axial fields as low as 0.06 Oe or 0.08 Oe. A control experiment on pure MnF_2, performed

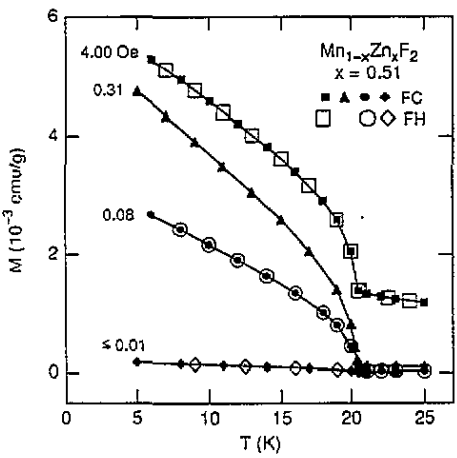

Figure 1. Temperature variation of the magnetization M for $x = 0.51$, measured in various fixed axial magnetic fields. FC data are for cooling in a fixed field, while FH data are for heating in a fixed field after cooling in the same field.

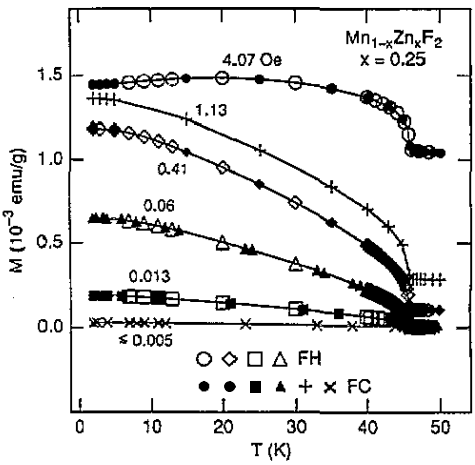

Figure 2. Temperature variation of the magnetization M for $x = 0.25$, measured in various fixed axial fields. Both FC and FH data are shown.

at $H_{axial} = 0.33$ Oe, did not reveal any rise of M below T_N. Thus, the magnetization rise is associated with the disorder introduced by the partial replacement of Mn by Zn.

The rise of M below T_N is for the *axial* magnetization; if a rise in the magnetization component perpendicular to the easy axis exists, it is much smaller. This result, obtained from measurements of the transverse moment, indicates that the remanent moment below T_N is parallel, or nearly parallel, to the easy axis. At first glance this conclusion may seem obvious since the sample was cooled in an applied axial field. However, besides the axial field there was also a field component perpendicular to the easy axis (due to the ever-present earth field). This perpendicular field, $H_{E\perp} \sim 0.1$ Oe, did not produce a comparable transverse remanent magnetization below T_N.

As noted in section 2, delays of 5–15 min were introduced between successive temperatures, in addition to the automatic delays of a system. Following such a delay, M was independent of time, at least up to ~ 1 h. All data shown here are after such delays.

3.2. Thermoremanent magnetization

Above T_N the axial magnetization M at all fields ($H < 23$ Oe and also $H = 2, 4$ kOe) is equal to $\chi_\parallel H_{axial}$, where $\chi_\parallel$ is the 'parallel' susceptibility along the easy axis. This ordinary contribution is expected to persist below T_N. It is therefore reasonable to try to represent the magnetization below T_N as a sum of two terms

$$M = M_r + \chi_\parallel H_{axial} \tag{1}$$

where M_r is some remanent magnetization. The data in figures 1 and 2 strongly suggest that well below T_N the contribution of M_r dominates if H_{axial} is below ~ 1 Oe, but at 4 Oe the contribution of $\chi_\parallel H_{axial}$ is already appreciable. As shown later, M_r becomes nearly saturated at ~ 1 Oe so that at much higher fields the contribution $\chi_\parallel H_{axial}$ should dominate. In the present work, $\chi_\parallel(T)$ was obtained from values of M/H_{axial} at 2 kOe and 4 kOe, where $\chi_\parallel H_{axial} \gg M_r$. The values of $\chi_\parallel$ obtained at 2 kOe and 4 kOe were practically identical.

Support for equation (1) and the precise meaning of M_r emerge from data for the isothermal magnetization as a function of H_{axial}. Such data were taken below 23 Oe following a slow cool down in a fixed field from $T > T_N$ to the final temperature. Examples of such data for both samples are shown in figures 3 and 4. There is no hysteresis in these results. Each of the isothermal magnetization curves is a straight line, with a slope in close agreement with the value of $\chi_\parallel$ at that temperature (as obtained at 2 kOe and 4 kOe). The intercept of the straight line with the magnetization axis is, by definition, the TRM, i.e., the value of M that remains after cooling in a constant field and then removing the field. The results in figure 3 and 4 therefore show that the isothermal magnetization obeys equation (1), and that M_r in that equation can be identified as the TRM. This M_r depends on the value of H_{axial} at which the sample was cooled, and on the final temperature to which the sample was cooled, i.e. $M_r = M_r(H_{axial}, T)$.

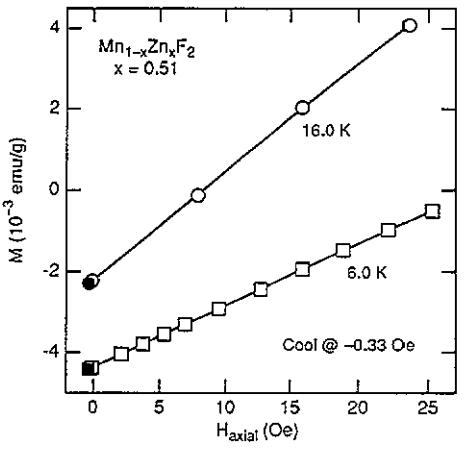

Figure 3. Isothermal magnetization M for $x = 0.51$ as a function of the axial field H_{axial}. Data at each temperature were taken after cooling from above T_N in a fixed axial field of -0.33 Oe. The filled square and filled circle are the data points for $H_{axial} = -0.33$ Oe. The straight lines are fits to (1).

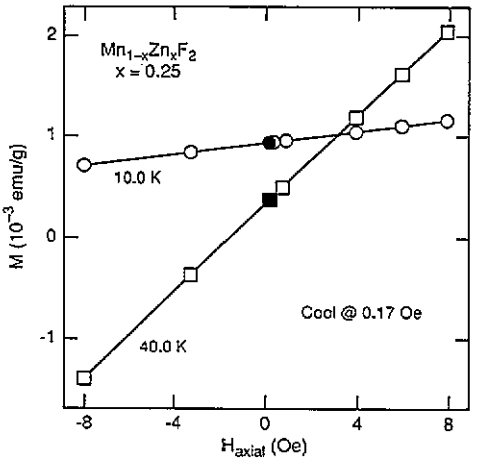

Figure 4. Isothermal magnetization for $x = 0.25$ as a function of the axial field. Data at each temperature were taken after cooling from above T_N in a fixed axial field of $+0.17$ Oe. The filled square and filled circle are the data for $H_{axial} = 0.17$ Oe. The straight lines are fits to (1).

Curves for M_r as a function of T at various constant values of H_{axial} were obtained by using equation (1). The input data were (a) results for the raw magnetization M versus T at constant H_{axial}, as in figures 1 and 2, and (b) values for $\chi_\parallel(T)$ measured at 2 kOe and 4 kOe. Figures 5 and 6 show the curves for M_r versus T corresponding to figures 1 and 2, respectively. It is clear that at any fixed T, M_r increases with H_{axial}. However, the rate at which M_r increases with field is much smaller above ~ 0.4 Oe than at much lower fields.

3.3. Sign and field dependence of M_r

For $|H_{axial}| \geqslant 0.02$ Oe the sign of M_r always agreed with that of H_{axial}. For lower fields, however, the results were somewhat ambiguous. When the uncorrected indium calibration of H_{axial} was used, the sign reversal of M_r occurred not exactly at zero field but at a few millioersted. For the reasons discussed in section 2 (misalignment of the c axis relative to the magnet's bore, and the 'crosstalk'), we attributed the latter result to a small offset

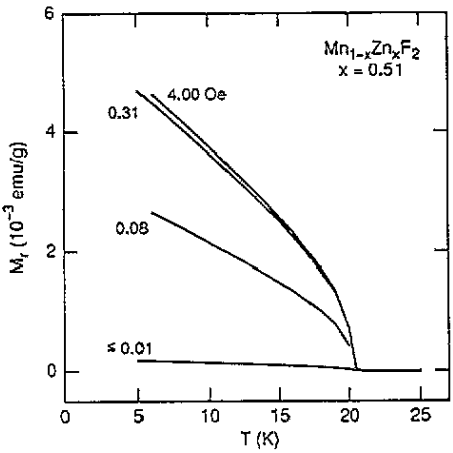

Figure 5. Temperature dependence of the thermoremanent magnetization M_r for $x = 0.51$ at various fixed axial fields. These results were obtained using the data in figure 1 and (1).

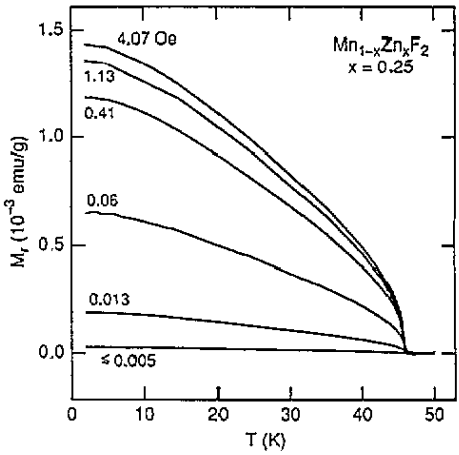

Figure 6. Temperature dependence of M_r for $x = 0.25$ at various fixed axial fields. These results were obtained using the data in figure 2 and (1).

error in the indium calibration. The calibration was then shifted so that the reversal of M_r occurred exactly at $H_{axial} = 0$.

Figure 7 shows results for M_r versus T, obtained from a series of runs at 14 different values of H_{axial}. These data are for $x = 0.51$. The same data can be represented alternatively as curves for M_r versus H_{axial} at various fixed temperatures. One such curve, for $T = 5.0$ K, is shown in the main part of figure 8. (The data collapse discussed later implies that results at different fixed temperatures differ only by a scale factor.) The inset in figure 8 shows an expanded view of the dependence of M_r on H_{axial} at low H_{axial} for three temperatures. Both figures 7 and 8 use the corrected indium calibration for the axial field. The difference between the corrected and uncorrected indium calibrations for this set of data was 0.008 Oe.

The data in figure 8 show that M_r is linear in H_{axial} at low H_{axial}, but is approaching saturation in fields as low as ~ 0.25 Oe. The latter result is consistent with data in figure 5 which show only a small change of M_r between 0.3 and 4.0 Oe. These results are for $x = 0.51$. The data in figure 6 indicate that for the other sample, with $x = 0.25$, M_r is practically saturated above ~ 1 Oe.

3.4. Data collapse

Analysis of the data for a given sample indicates that all the curves for M_r versus T (at various H_{axial}) are the same except for a scale factor. That is, if the curves for M_r versus T are all normalized to unity at one fixed temperature then all the curves become identical. Figure 9 shows such a data collapse for $x = 0.51$. After a normalization at 5.0 K, the 14 data sets in figure 7, measured between -0.014 Oe and $+0.23$ Oe, have collapsed into a single curve. A similar data collapse for $x = 0.25$ is shown in figure 10. Here, five data sets in figure 6 have collapsed into a single curve, after a normalization at 7.0 K.

Figures 9 and 10 show data collapse for each sample separately. However, by using the reduced temperature $t \equiv T/T_N$ instead of T, one can collapse the data for *both* samples into a single curve. This is illustrated by the results in figure 11 which compares data for $M_r(t)/M_r(t = 0.24)$ versus t in both samples. The results in figures 9–11, taken together,

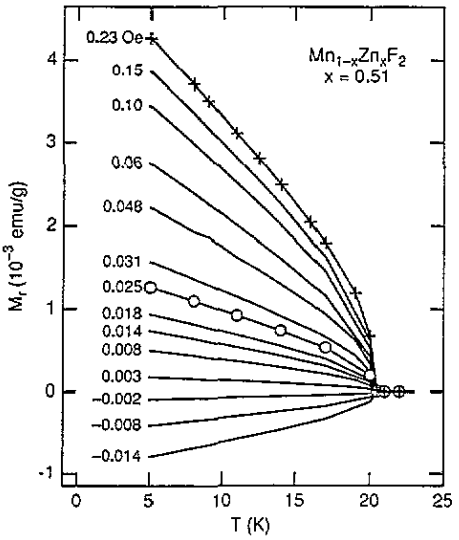

Figure 7. Temperature dependence of M_r at fixed values of the axial field, from −0.014 to +0.23 Oe. These data are for $x = 0.51$. To avoid overcrowding, data points are shown only for two curves.

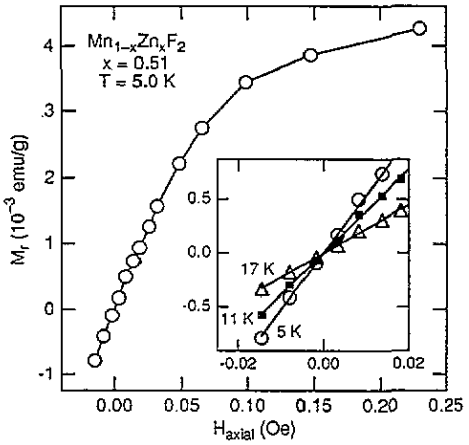

Figure 8. Dependence of M_r on H_{axial} at $T = 5.0$ K. These results are based on figure 7. The inset shows the dependence of M_r on H_{axial} at very low axial fields. Data in the inset are for three fixed temperatures.

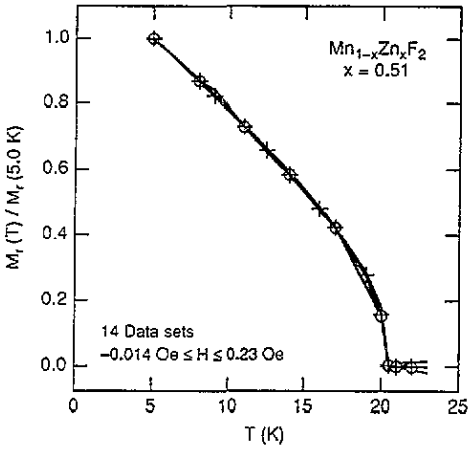

Figure 9. Temperature dependence of the normalized TRM $M_r(T)/M_r(5.0\text{ K})$ for $x = 0.51$. All 14 data sets in figure 7 are included in this plot. The data points correspond to data points in figure 7.

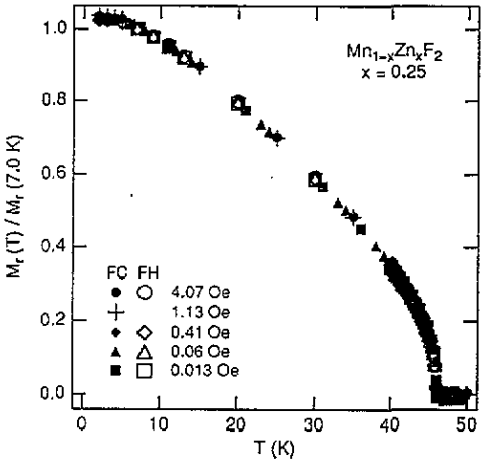

Figure 10. Temperature dependence of the normalized TRM $M_r(T)/M_r(7.0\text{ K})$ for $x = 0.25$. These data, for five different fixed axial fields, correspond to the data in figures 2 and 6.

indicate that if the reduced temperature t is used then all curves for M_r versus t are the same in both samples, except for a scale factor.

In addition to the $Mn_{1-x}Zn_xF_2$ system discussed in this paper we have also been studying antiferromagnets of the chemical formulas $K_2Fe_{1-x}In_xCl_5{\cdot}H_2O$ and $K_2Fe(Cl_{1-x}Br_x)_5{\cdot}H_2O$. The magnetic ion Fe^{3+}, in the latter two systems, has a spin $S = \frac{5}{2}$, i.e., the same as that of Mn^{2+}. Preliminary results indicate that if the reduced temperature t is used then the

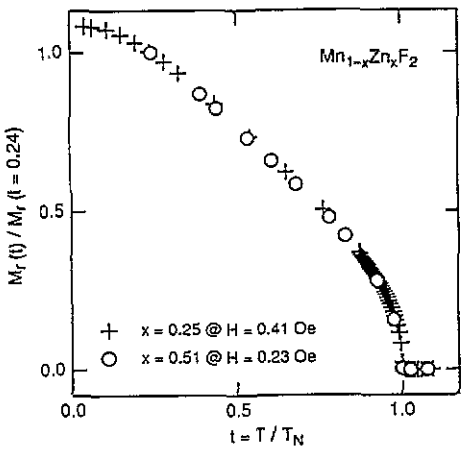

Figure 11. Normalized TRM as a function of the reduced temperature $t \equiv T/T_N$. Two data sets, one for $x = 0.25$ at $H_{axial} = 0.41$ Oe and the other for $x = 0.51$ at $H_{axial} = 0.23$ Oe, are compared. For both data sets, $M_r(t)$ was normalized to the value at $t = 0.24$.

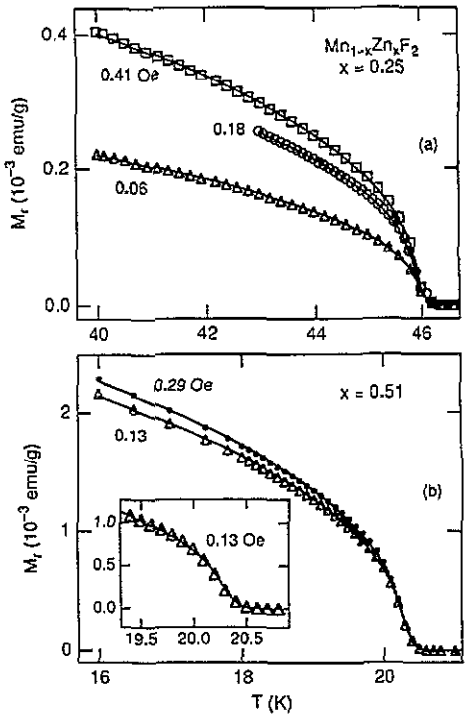

Figure 12. Temperature variation of M_r near the Néel temperature: (*a*) data for $x = 0.25$ at three values of H_{axial}; (*b*) data for $x = 0.51$. The inset gives an expanded view of the data for 0.13 Oe very near T_N. The full curves are best fits to (3).

shapes of all the curves $M_r(t)/M_r(0)$ versus t for $K_2Fe_{1-x}In_xCl_5 \cdot H_2O$ are the same as those for $Mn_{1-x}Zn_xF_2$. On the other hand, a different dependence of M_r on t is observed in $K_2Fe(Cl_{1-x}Br_x)_5 \cdot H_2O$. One possible reason for this behaviour is that both $Mn_{1-x}Zn_xF_2$ and $K_2Fe_{1-x}In_xCl_5 \cdot H_2O$ are random-site antiferromagnets, whereas $K_2Fe(Cl_{1-x}Br_x)_5 \cdot H_2O$ is a random-bond antiferromagnet. The results on the antiferromagnets containing Fe^{3+} will be published later.

3.5. Effective critical exponent

Detailed data for M_r near T_N were taken. The three data sets for $x = 0.25$ are shown in figure 12(*a*). Among these, the data at 0.06 Oe and 0.41 Oe are FH data, but those at 0.18 Oe include both FC and FH data. The data for $x = 0.51$ are shown in figure 12(*b*). Each of the two data sets in figure 12(*b*) includes both FC and FH data.

If M_r is governed by a critical exponent β_r, then the results for M_r versus T, at constant H_{axial} near T_N, should obey the equation

$$M_r = A(1 - T/T_N)^{\beta_r} \tag{2}$$

where A is a constant. In fitting the T dependence of M_r it was necessary to allow for an apparent broadening of the transition. This apparent broadening can be seen in the inset of

figure 12(*b*). (We call it an 'apparent broadening' because it is yet to be established that the observed small 'tail' in M_r versus T is caused by a variation of T_N within the sample; it is conceivable that it is an intrinsic property of M_r.) To include the apparent broadening in the fit, a Gaussian variation of T_N within the sample was assumed [10]. The equation for the fit was therefore

$$M_r(T) = C\int_T^\infty \left(1-\frac{T}{T_N}\right)^{\beta_r} \exp\left[-\frac{1}{2}\left(\frac{T_N-\bar{T}_N}{\sigma}\right)^2\right] dT_N. \tag{3}$$

The mean Néel temperature $\bar{T}_N$, the standard deviation σ of the Gaussian, β_r and C were treated as adjustable parameters. The results for these parameters were studied as a function of the range of temperatures included in the fit. A particular range covered all $M_r(T)$ above some minimum temperature T_{min}.

The results for β_r as a function of the width T_N–T_{min} of the range are shown in figure 13. Figure 13(*a*) is for the three data sets for $x = 0.25$, while figure 13(*b*) is for $x = 0.51$. In all cases there is a significant increase of β_r as the width of the range increases. Extrapolations that assume a smooth dependence of β_r on range suggest the following estimates for β_r in the limit of zero range: $\beta_r = 0.375 \pm 0.025$ for $x = 0.25$, and 0.385 ± 0.015 for $x = 0.51$. For $x = 0.25$ all the results for $\bar{T}_N$ were between 45.96 K and 46.04 K, while for $x = 0.51$ all values for $\bar{T}_N$ were between 20.30 K and 20.33 K. Values of σ were near 0.1 K for both samples.

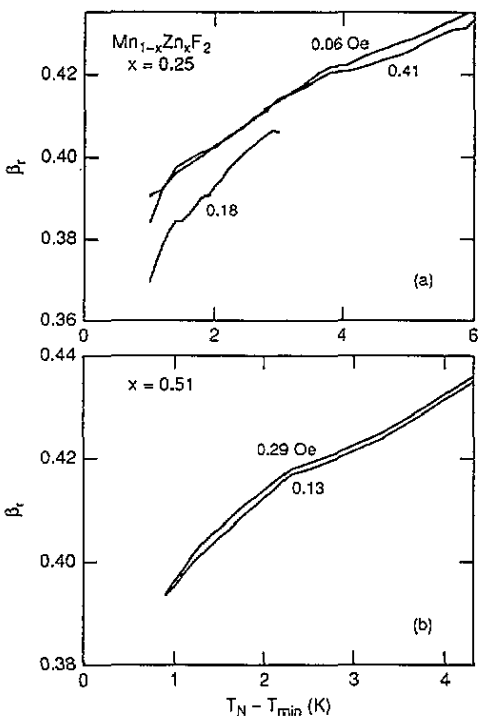

Figure 13. Values of β_r obtained from fits to (3) plotted as a function of the width $T_N - T_{min}$ of the temperature range included in the fit: (*a*) results for $x = 0.25$, corresponding to the data in figure 12(*a*); (*b*) results for $x = 0.51$, corresponding to the data in figure 12(*b*).

The significance of the exponent β_r is unclear. As discussed later, the temperature variation of M_r over a wide range does not agree with that of the staggered magnetization.

Thus, the value of β_r near T_N may not be equal to the exponent β for the long-range order parameter. The theoretical value of β for the random-exchange Ising model is 0.35 [13, 14]. The experimental results of β in the $Mn_{1-x}Zn_xF_2$ system at $H = 0$ are $\beta = 0.35 \pm 0.01$ from NMR [15], and 0.35 ± 0.03 and 0.33 ± 0.02 from x-ray scattering [10, 12]. The latter two values are for the same boules as used in the present work. The width of the transition observed in the x-ray-scattering experiments was much smaller than that observed in the present work, despite the fact that the same boules were used. The probable reason for the difference in width is that the volume scanned by the x-ray beam was orders of magnitude smaller, which minimized composition variations.

3.6. Field-switching experiments

Previously we discussed experiments in which H_{axial} was kept constant while cooling from above T_N down to the lowest temperature (FC procedure). In such experiments $M_r(T)$ depended on H_{axial}. We now focus on experiments of a different type: the sample is first cooled in an axial field H_1 to some temperature T_s below T_N, but at T_s the axial field is switched to H_2. Following the field change, the sample is cooled further at H_2. After reaching the lowest temperature, the sample is heated in the same H_2 to a temperature above T_N. The results for M obtained from these experiments were analysed using (1). The main conclusion is that M_r, as deduced from equation (1), is unaffected by the field switch. The values of $M_r(T)$ in the field H_2 continue to follow the curve that would have been obtained had the field remained at H_1. That is, despite the field switch, M_r continues to be governed by the field $H_1 \equiv H_{axial}(T_N)$ at which the sample was cooled through T_N. This conclusion was verified for axial fields up to ~ 1 Oe; switching from/to higher fields was not attempted.

Figure 14 shows some of the data for $x = 0.51$. The filled squares connected by a broken curve were all taken at -0.31 Oe while cooling from above T_N to 5 K. This usual FC procedure was used in this case in order to determine the curve of M_r versus T for cooling at $H_{axial} = -0.31$ Oe. Such a curve is needed for a comparison with field-switched data. The field switched data are represented by the full curve in figure 14. Here, the axial field was switched from $H_1 = -0.31$ Oe to $H_2 = +1.48$ Oe at $T_s = 20.0$ K. (This switching temperature is only 0.3 K below the mean Néel temperature $\bar{T}_N$.) The filled circles on the full curve are data taken while cooling after the field switch. The open circles are data taken while heating at the same H_2, after the two-stage cool down (first to 20 K at H_1, and then to 5 K at H_2). All the data in figure 14 are for M, i.e., not for $M_r = M - \chi_\parallel H_{axial}$.

A comparison between the full and broken curves in figure 14 shows that the field switch had only a small effect on M. A full analysis using equation (1) indicates that the remanent magnetization $M_r(T)$ is the same for both full and broken curves of this figure, i.e., the small difference between these curves is completely accounted for by the term $\chi_\parallel H_{axial}$ in equation (1). Thus, changing the field below T_N has no effect on M_r; the field $H_1 \equiv H_{axial}(T_N)$ that was present when cooling through T_N remains in control of $M_r(T)$.

Data for $x = 0.25$ are shown in figure 15. These results are for M_r, i.e., the contribution $\chi_\parallel H_{axial}$ to M has already been subtracted. The broken curve represents FC data in a single field, $H_{axial} = +0.06$ Oe, starting above T_N and ending at 10 K. The full curve represents field-switched data: the field was switched at $T_s = 44.0$ K from $H_1 = +0.06$ Oe to $H_2 = -0.10$ Oe. To avoid confusion, individual data points have been deleted in figure 15, and only results for cooling after the field switch are shown. (Data for heating at H_2 after the two-stage cool down to 10 K also follow the full curve, but they extend to higher temperatures.) It is clear that changing the field below T_N has a negligible effect on M_r.

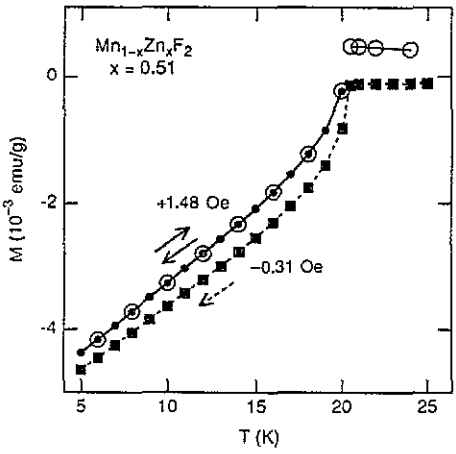

Figure 14. Temperature dependence of the magnetization M for $x = 0.51$. The filled squares on the broken curve were obtained while cooling from above T_N in an axial field of −0.31 Oe (i.e., the normal FC procedure). The filled and open circles on the full curve are field-switched data. They were obtained after cooling from above T_N to 20.0 K at $H_1 = -0.31$ Oe, and then switching to $H_2 = +1.48$ Oe. The filled circles correspond to cooling from 20K to 5K after the field switch. The open circles correspond to heating from 5 K at 1.48 Oe after the two-step cool down (first to 20 K at −0.31 Oe, and then to 5 K at 1.48 Oe).

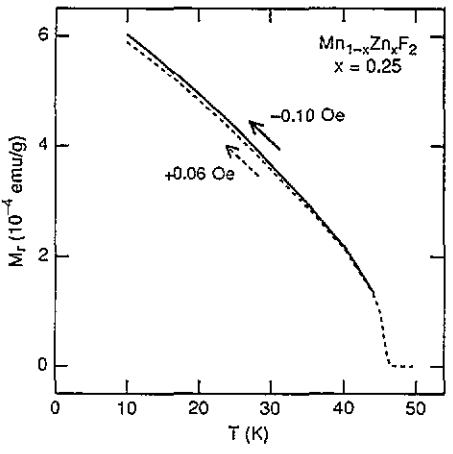

Figure 15. Temperature dependence of M_r for $x = 0.25$. The broken curve represents data obtained while cooling from above T_N at +0.06 Oe, i.e., the usual FC procedure. The full curve represents field-switched data, obtained while cooling after a field switch at 44.0 K from $H_1 = +0.06$ Oe to $H_2 = -0.10$ Oe.

Note that both in this example and in that in figure 14 the field switch involved a change of the *sign* of H_{axial}; still there was no effect on M_r.

Earlier, the value of M_r deduced from FC data using (1) was shown to be equal to the TRM. The results of the field-switching experiments, and also the results for the isothermal magnetization (e.g., figures 3 and 4), imply that this M_r is also equal to the excess magnetization ΔM. By definition, $\Delta M = M_{FC} - M_{ZFC}$. Cooling in an axial field H_0 to a temperature T gives

$$M_{FC}(H_0, T) = M_r(H_0, T) + \chi_{\parallel}(T)H_0. \tag{4}$$

Cooling at zero field to temperature T leads to a vanishing M_r which does not change when the field is increased to H_0. Thus, $M_{ZFC}(H_0, T) = \chi_{\parallel}(T)H_0$. The difference $\Delta M(H_0, T)$ is therefore equal to $M_r(H_0, T)$, at least for fields up to several oersteds. The IRM is zero at these low fields.

4. Discussion

The remanent magnetization studied here exists only below T_N. Therefore, it is related to the antiferromagnetic order, and is not a spurious effect caused by ferromagnetic precipitates. Since no remanent magnetization was found in pure MnF_2, the cause of the remanent magnetization must be the partial replacement of Mn by Zn.

The physical origin of the remanent magnetization at very low fields is still unknown. Earlier studies focused on the behaviour at much higher magnetic fields [4–6, 16–19]. The excess magnetization observed in these earlier studies was attributed to random fields. Such random fields, which are generated by H [3], are known to lead to the formation of domains in FC experiments. The domains contribute to the excess magnetization in two ways. First, there is a surface effect, which is the excess magnetization in the domain walls. Second, there is a volume effect, which is the excess magnetization due to the difference between the numbers of 'up' and 'down' spins in any given domain. The latter difference is caused by the random statistical distribution of the magnetic ions over the larger number of available cation sites. It is energetically preferable for that sublattice with more spins (majority sublattice) to have its magnetic moment parallel to H rather than antiparallel to H. Therefore, a net magnetization parallel to H is produced.

Both the surface and the volume contributions to the excess magnetization should increase when the average domain size R decreases. Because R decreases with increasing H (stronger random field), the excess magnetization is predicted to increase rapidly with H [5, 6, 16, 17]. This predicted increase is observed in high fields, but is in sharp contrast with the behaviour observed in the present work at low fields. In these low fields, M_r already approaches saturation at ~ 1 Oe. Thus, random fields do not explain the present observations. The same conclusion can also be reached by considering the domain size R on the assumption that this size is governed by the random field: Extrapolation of the H dependence of the FC domain size for $x = 0.25$, reported in [10], indicates that for $H \simeq 1$ Oe the domain size is orders of magnitude larger than the size of our samples. The explanation of the present data in terms of random fields is therefore not viable; the random field at $H \simeq 1$ Oe is far too weak.

Random fields generated by H are not the only cause of antiferromagnetic domains. It is well known that antiferromagnetic domains exist even at low (or zero) magnetic field [20–22]. In the case of MnF_2 adjacent domains have opposite directions for the staggered magnetization, i.e., the sublattice magnetizations are interchanged [22]. The possibility that the observed remanent magnetization at low fields is caused by such domains was considered. As in the models involving random fields, possible contributions to the domain magnetization are (1) a surface effect, due to the domain walls, and (2) a volume effect, due to the imbalance between the numbers of up and down spins.

A domain model based on the volume contribution (DV model) was considered in some detail. It was assumed that the domain configuration is frozen below T_N, i.e., domain walls cannot move and the staggered magnetization in a domain cannot reverse its direction. This assumption was made in order to explain the field-switching experiments. An explanation of data collapse for a single sample also follows from this assumption, as will be discussed shortly. To explain the dependence of M_r on the axial field $H_{axial}(T_N)$ present while cooling through T_N, the following physical picture was assumed. The volume contribution arises because the two sublattices in a given domain have unequal numbers of spins. As already stated, the difference is assumed to arise from the statistics of the random distribution of the magnetic ions over the cation sites. The net domain magnetic moment is parallel to the moment of the majority sublattice. The direction of the magnetic moment of the majority sublattice, whether parallel or antiparallel to H_{axial}, is decided when cooling through T_N. Statistically, this decision is influenced by the difference between the Zeeman energies of the domain for the two possible directions of the majority sublattice moment relative to H_{axial}. A stronger axial field creates a stronger preference for the majority sublattice to have its magnetic moment parallel to H_{axial}. Once the direction of the moment of the

majority sublattice is decided near T_N, the decision cannot be reversed without warming the sample above T_N (frozen domains).

Although the above version of the DV model explains some of the salient features of the data, several basic predictions that follow from such a model are contradicted by the data. One prediction is that the temperature dependence of M_r for any value of $H_{axial}(T_N)$ is the same as that for the sublattice magnetization M_s. The reason is that both the domain net magnetic moment and the sublattice magnetization are proportional to the average moment $\langle\mu_z\rangle$ per spin. The domain magnetic moment m_d is the product of $\langle\mu_z\rangle$ and the difference Δn between the numbers of spins on the up and down sublattices. In the present version of the DV model the values of Δn for the various domains are frozen below T_N. Thus, for any $H_{axial}(T_N)$ the remanent magnetic moment of the sample as a whole is given by

$$M_r = \sum m_d = \sum \Delta n \langle\mu_z\rangle = \langle\mu_z\rangle \sum \Delta n \tag{5}$$

which is proportional to $\langle\mu_z\rangle$. Since M_s is also proportional to $\langle\mu_z\rangle$, it follows that $M_r(T)$ is proportional to $M_s(T)$. This result holds for M_r at any $H_{axial}(T_N)$. Data collapse for a single sample then follows, i.e., $M_r(T)/M_r(0)$ does not depend on $H_{axial}(T_N)$.

Data collapse for a single sample is observed experimentally, but the proportionality between M_r and M_s is not obeyed. The dependence of M_s on T has been measured over a wide temperature range using x-ray scattering [12, 16]. These data for $M_s(T)$ are for the same two boules that were used in the present work. They were compared with the present data for $M_r(T)$. For both $x = 0.25$ and 0.51, the T dependence of M_r is noticeably different from that of M_s.

Other difficulties with the DV model arise when the average domain size is estimated on the basis of this model. Let the number of cation sites for an average domain be $2N$, so that there are N cation sites per sublattice in an average domain. The probability that n of these N sites are occupied by magnetic ions is given by the binomial distribution. The mean number of Mn spins on each sublattice is $\bar{n} = N(1-x)$, and the standard deviation for n is

$$\sigma_n = [Nx(1-x)]^{1/2}. \tag{6}$$

A typical excess magnetic moment m_d per domain should have an approximate magnitude of $\sigma_n\langle\mu_z\rangle$. That is, a typical $|\Delta n|$ is approximately σ_n. The sublattice magnetic moment per domain is $\bar{n}\langle\mu_z\rangle$. In FC experiments with $H_{axial} > 0.3$ Oe (near saturation) the magnetic moments of all the domains are aligned parallel to the applied field, i.e., in all the domains the magnetic moment of the majority sublattice is parallel to H_{axial}. In that case, all Δn have the same sign. If there are D domains per gram, then the ratio between the remanent magnetic moment per gram and the sublattice magnetic moment per gram is

$$\frac{M_r}{M_s} = \langle\mu_z\rangle \sum \Delta n \Big/ D\bar{n}\langle\mu_z\rangle \cong \frac{\langle\mu_z\rangle D\sigma_n}{D\bar{n}\langle\mu_z\rangle}. \tag{7}$$

Thus, above about 0.3 Oe,

$$M_r/M_s \cong \sigma_n/\bar{n} = [x/N(1-x)]^{1/2}. \tag{8}$$

For $x = 0.5$ above 0.3 Oe, the extrapolated value of M_r at $T = 0$ is 5×10^{-3} emu g^{-1}. The calculated M_s at $T = 0$ is 71 emu g^{-1}. Equation (8) then gives $N \cong 2 \times 10^8$ for an average domain. The difficulty with this estimate is that according to [12] the average domain size

at 'zero field' in a sample from the same boule is at least 4 μm, or 10^4 lattice constants. Thus N should exceed $\sim 10^{12}$. Another difficulty with this estimate for N is that it leads to too low a value of m_d to cause the domains to be aligned near T_N at 0.3 Oe. From the field switching experiments it follows that the alignment is already completed at 20 K. For this to be the case, $m_d H_{axial}/k_B T$ should be of the order of unity or larger at 0.3 Oe and 20 K. But the estimate for N, supplemented by the measured T dependence of M_r which reflects that of m_d (in the DV model) leads to a ratio $m_d H_{axial}/k_B T \sim 10^{-2}$.

The discussion above strongly suggests that a domain model based on the volume contribution is incapable of explaining the present data. It is possible that a domain model based on the surface contribution (from domain walls) will be more successful. Thus far we have found no simple way of testing the latter model. Of course, it is possible that the solution to the problem lies in an entirely different direction.

Acknowledgments

The work at Tufts University was supported by NSF grant DMR-9219727. The equipment in the Magnetometry Facility at Tufts was donated by the W M Keck Foundation. The work at the University of São Paulo (USP) was supported by CNPq, BID, and FAPESP under grant 92/0845-2. The work of the University of Zaragoza was supported by CICYT grant MAT91-681 and Programa de Cooperación Cientifica Iberoamericana. The cooperation between Tufts University and USP is supported by NSF grant INT-9216424 and by CNPq.

References

[1] Fries T, Shapira Y, Paduan-Filho A, Becerra C C and Palacio F 1993 *J. Phys.: Condens. Matter* **5** L107
[2] Paduan-Filho A, Barbeta V B, Becerra C C, Gabas M and Palacio F 1992 *J. Phys.: Condens. Matter* **4** L607
[3] Fishman S and Aharony A 1979 *J. Phys. C: Solid State Phys.* **12** L729
[4] Ikeda H and Kikuta K 1983 *J. Phys. C: Solid State Phys.* **16** L445
[5] Pollak P, Kleemann W and Belanger D P 1988 *Phys. Rev.* B **38** 4773
[6] Leitão U A, Kleemann W and Ferreira I B 1988 *Phys. Rev.* B **38** 4765
[7] Shapira Y, Oliveira N F Jr and Foner S 1984 *Phys. Rev.* B **30** 6639
[8] Birgeneau R J, Shapira Y, Shirane G, Cowley R A and Yoshizawa H 1986 *Physica* B **137** 83
[9] Cowley R A, Shirane G, Yoshizawa H, Uemura Y J and Birgeneau R J 1989 *Z. Phys.* B **75** 303
[10] Hill J P, Feng Q, Birgeneau R J and Thurston T R 1993 *Phys. Rev. Lett.* **70** 3655; *Z. Phys.* at press
[11] Mitchell P W, Cowley R A, Yoshizawa H, Böni P, Uemura Y J and Birgeneau R J 1986 *Phys. Rev.* B **34** 4719
[12] Thurston T R, Peters C J, Birgeneau R J and Horn P M 1988 *Phys. Rev.* B **37** 9559
[13] Newman K E and Riedel E K 1982 *Phys. Rev.* B **25** 264
[14] Jug G 1983 *Phys. Rev.* B **27** 609
[15] Dunlap R A and Gottlieb A M 1981 *Phys. Rev.* B **23** 6106
[16] Hill J P 1992 *PhD Thesis* MIT
[17] Nattermann T and Vilfan I 1988 *Phys. Rev. Lett.* **61** 223
[18] Han S-J, Belanger D P, Kleemann W and Nowak U 1992 *Phys. Rev.* B **45** 9728
[19] Lederman M, Selinger J V, Bruinsma R, Hammann J and Orbach R 1992 *Phys. Rev. Lett.* **68** 2086
[20] Farztdinov M M 1964 *Usp. Fiz. Nauk.* **84** 611 (Engl. Transl. 1965 *Sov. Phys.–Usp.* **7** 855)
[21] Farztdinov M M 1964 *Fiz. Metal. Metalloved.* **19** 321 (Engl. Transl. 1965 *Phys. Met. Metallog.* **19** 1)
[22] Alperin H A, Brown P J, Nathans R and Pickart S J 1962 *Phys. Rev. Lett.* **8** 237